33RD CONGRESS
OF THE INTERNATIONAL COUNCIL
OF THE AERONAUTICAL SCIENCES
STOCKHOLM, SWEDEN, 4-9 SEPTEMBER, 2022

ICAS 2022 SWEDEN

DEVELOPMENT OF A CONCEPTUAL DESIGN TOOL TO PREDICT PERFORMANCE OF HYDROGEN FUELLED PRECOOLED AIR-BREATHING ROCKET ENGINES

Giovanni Grimaldi[1]

[1]MSc graduate in Aerospace Engineering and Specializing Master student at Politecnico di Torino

Abstract

The scope of this work is to create propulsive models for assessing the performance of a new type of hydrogen fuelled engine which are the precooled air-breathing rocket engines. One current example of this type of propulsive architectures is the SABRE, under design at Reaction Engines Ltd. Thus, in the following, starting from a review of the architecture of the engine and of other models, different cycles will be presented and tested against the data published on SABRE to prove their validity and applicability in initial conceptual phases of design, when not many inputs are known and different alternatives must be compared nimbly.

Keywords: MORE&LESS Academy, propulsion modeling, pre-cooled engines, SABRE engine, hydrogen

1. Introduction and research background

Lately, many different propulsive architectures are developed every day and one promising category is that of precooled engines. One leader producer in this field is the UK company Reaction Engines Ltd, which is currently designing the SABRE and the derived engine Scimitar. In particular, SABRE is an acronym that stands for Synergetic Air-Breathing Rocket Engine and has the objective of powering the proprietary spaceplane Skylon, which could revolutionize the access to space in an inexpensive, reliable and reusable way [1]. SABRE has the peculiarity of being able to operate as a precooled air-breathing engine for the first part of the ascent, exploiting the thick, dense air of the atmosphere as an oxidizer. After reaching an altitude of 25 km, the intake is closed and a mixture of hydrogen and on-board oxygen is burnt in the rocket chamber to produce thrust. Moreover, even if initially applied for the space access, the technology behind the functioning of SABRE during the air-breathing phase is believed to be revolutionary in many different fields, in particular aeronautics. One of the current challenges of civil aviation is to bring together supersonic civil transport and lower costs, high reliability and low environmental impact. In order to do so, hydrogen is believed to be one of the best possibilities when coming to fuels. From these premises, the study by Reaction Engines on Scimitar is derived [2]. Scimitar is slightly different from SABRE and has different parameters regarding its components. However, a general study on SABRE is broadly applicable also to Scimitar and in future we will probably see more and more propulsive architectures using similar thermodynamic cycles.

The present work starts from these observations and aims at creating a model for estimating the propulsive performance of SABRE-like engines during the air-breathing phase. The main challenge was to develop models that could be reliable and accurate even if using an amount and type of data available in a conceptual design phase, during which usually not much is known about the engine of interest. Different models will be presented and the results calculated using SABRE characteristics in order to compare them to the performance parameters published by Reaction Engines. By doing so, the model is validated and can then be used with other entry parameters to simulate different engines. The considerations were made on SABRE because it is the first design produced by Reaction Engines and actual data are available. Moreover, once the propulsive characteristics of the engine are obtained, they can be used to assess the greenhouse and pollutant emissions of Skylon, the Reusable Access to Space Vehicle under study at Reaction Engines [3]. This choice has been made also because more emissions estimations exist for the Scimitar [4] but none was found about the SABRE while reviewing the technical literature and it is believed that this will be an important matter in future, due to the very strict predicted turnaround time of the Skylon, that will probably be able to make the number of annual space launches grow drastically.

1.1 Reference engine and aircraft

Before going to the actual description of the computational models, some details on Skylon and SABRE must be presented in order to give a better comprehension of the work done.

Regarding the Skylon, it is a fully reusable, Single Stage To Orbit spaceplane, currently under design at Reaction Engines. Its main characteristic is its ability to take off and land as a common airplane, thus simplifying the operations of access to space. Differently from designs of other spaceplanes, Skylon shows a clear division between the slender fuselage and the wing, that was proven to be optimum in terms of weight, lift and volume, though creating problems related to the fact that the wing does not fit entirely inside the bow shock at the reentry, determining high localized heat fluxes and the necessity of an active cooling system. In Figure 1, it can be seen how the greatest part of the fuselage is occupied by the hydrogen cryogenic tanks, while a minimum part is reserved for the liquid oxygen tanks, due to the fact that in the first part of the ascent the oxidizer is the outside air. The control of the spaceplane during the atmospheric phase is obtained by the use of the canard foreplanes, ailerons and aft fin, while in absence of air the control is obtained via the differential throttling and the nozzle gimbaling and through a Reaction Control System after the main engines shut off. The gross take-off mass is around 325 tons with a dry mass around 53 tons and the payload capacity is around 11 tons in the ISS orbit [3].

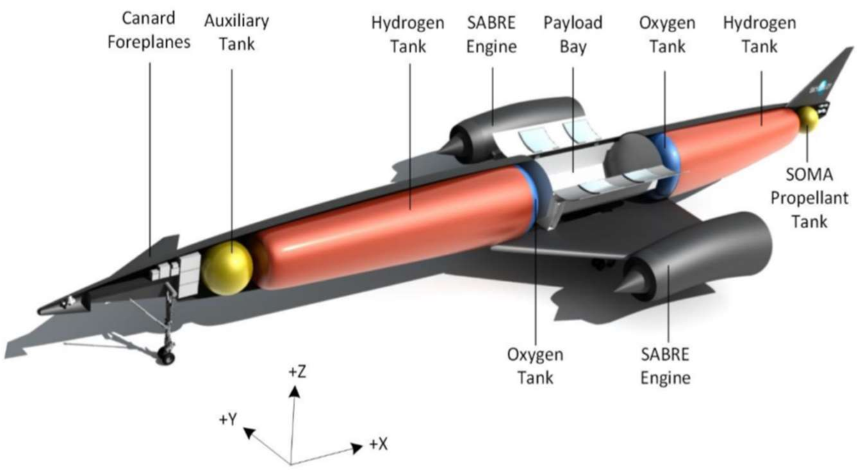

Figure 1 - Skylon layout (from [3])

The typical ascent trajectory is reported in Figure 3, both for the air-breathing and pure rocket phases [3]. From this, data were extrapolated for the assessment of ambient conditions during the air-breathing phase, which is the core of this work.

Skylon is powered by two SABRE engines mounted at the tip of the wings. The name of the plant is an acronym that stands for Synergetic Air-Breathing Rocket Engine and, much as Skylon is an evolution of British Aerospace HOTOL, it is derived by the corresponding liquid air cycle engine (LACE), however avoiding air liquefaction. In many ways, the engine allows to keep together the advantages of air breathing and rocket engines, respectively the low propellant consumption, since only the fuel mass is significant for the performance in the first phase, and the high delivered thrust, allowing for a great reduction of total weight. The engine cycle is reported in Figure 4 and, as it can be seen, it is a turbomachinery-based cycle, allowing the generation of static thrust, differently from a ramjet.

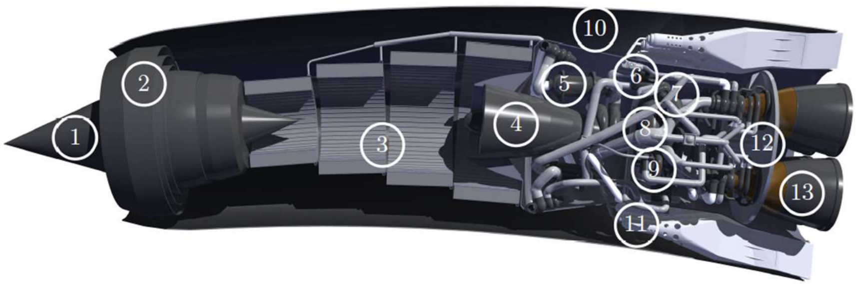

Figure 2 - From [5]: SABRE section: 1) movable spike 2) intake 3) precooler 4) air compressor 5) pre-burner and reheater (HX3) 6) helium circulator 7) H2 pump 8) He turbine and regenerator (HX4) 9) LOx pump 10) spill duct 11) ramjet burn

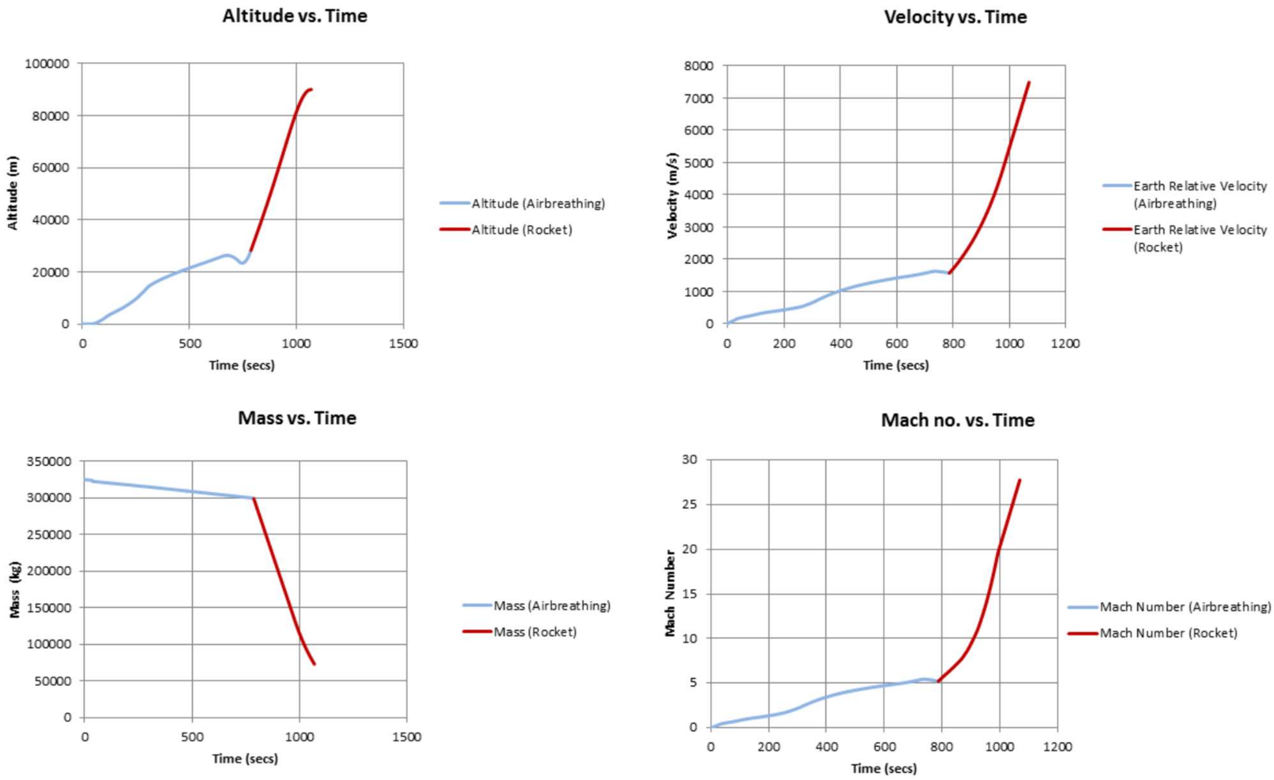

Figure 3 - trajectory of the typical mission of Skylon (from [3]).

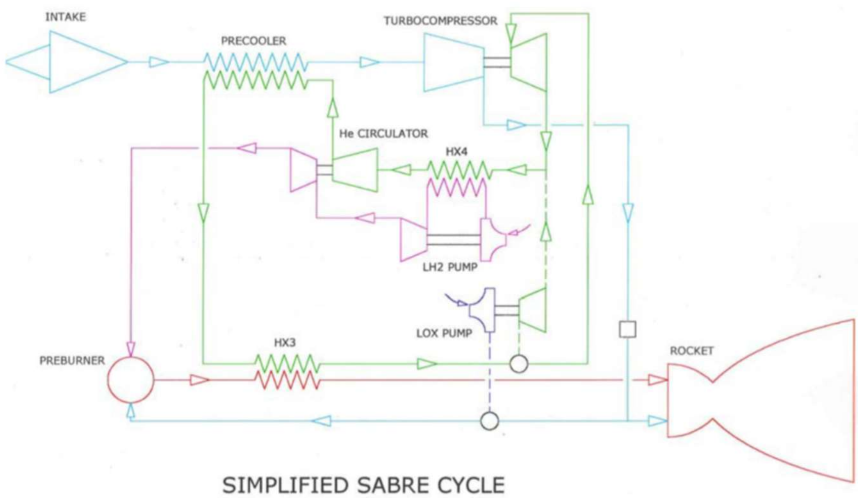

Figure 4 - SABRE cycle in both air breathing and rocket modes (from [6])

In the first mode, that is the one of interest for this work, the air captured by the intake is deeply cooled down before entering a high-pressure ratio compressor; after that the flow is split and a part goes to a pre-burner which, through the consequent heat exchanger allows, together with the precooler, to power the helium cycle. The remaining air is directly fed into the chamber which, thanks to the high compressor outlet pressures, can be a rocket type combustion chamber allowing to have an exit area lower than the intake area. This air cycle is supported by two other cycles: the hydrogen and the helium ones. The hydrogen is used as the fuel but also as the heat sink for the heat extracted by the precooler, through the HX4. The possibility of using the hydrogen directly facing the air cycle inside the PC was discarded due to hydrogen embrittlement problems thus introducing the necessity of the helium closed loop that serves to transfer the heat from the air to the hydrogen while also powering the air compressor. The helium is in fact strongly heated inside the precooler and slightly in the HX3, flowing then in the turbine mechanically linked to the compressor and then in the HX4 that transfer power to the hydrogen cycle which then powers the first turbine linked to the liquid fuel turbopump and then to the second turbine linked to the helium circulator.

The intake operates, when in supercritical mode, with a three shocks compression, the first at the tip of the movable spike, the second at the cowl before the throat and the third after the intake throat. The position of this last shock is controlled with the spillage of the flow to the bypass burners. These are introduced because the nacelle is designed to swallow the amount of air necessary for the core engine to operate at an altitude of 25 km: therefore, at lower altitudes and higher atmospheric densities, the ingested air is higher than necessary and must be bypassed. In order not to incur in a high drag penalty, some fuel is also bypassed and burnt in a ring of ramjet burners. This is possible because the engine runs with a very hydrogen rich mixture due to the cooling requirements. The nacelle then closes in the rocket phase to reduce drag.

However, the enabling technology of SABRE cycle is the precooler, which has been subject of the highest research interest by REL [7]. It is composed by an array of brazed microchannels made by Inconel cast alloy 718 in which the helium flows and cools down the outside air flow of roughly 400 kg/s from a temperature of 1250K to 100K. The low temperatures at the compressor inlet allow then for the high compression ratio of 140. Many problems are related to the precooler, one above all the possible formation of ice that could disturb the flow and cause unpredictable performances. However, the precooler has been successfully tested in late 2019 by REL, followed then by the successful testing of the pre burner and HX3 [8].

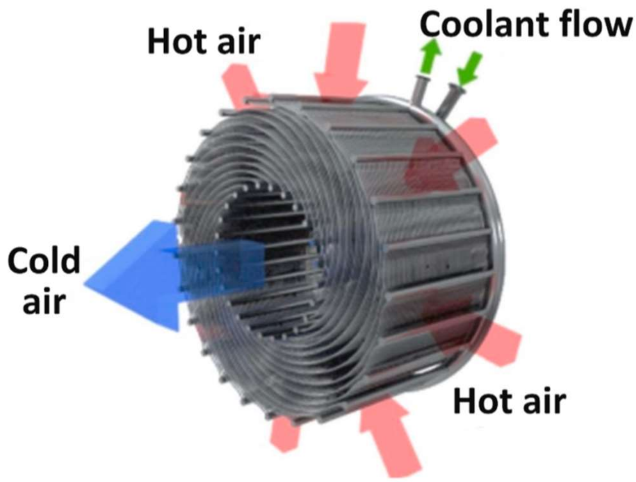

Figure 5 - Scheme of the SABRE precooler (from [9])

After the precooler the air goes in the compressor which is a relatively conventional three spools axial compressor powered by the counter rotating helium turbine, that can in turn power also the LOx turbopump during the rocket ascent. There is then the pre burner that, differently from classical staged combustion, is used as a heat source to top off the heat input in the helium cycle through the counterflow HX3 heat exchanger. The pre burner always operates in rich mixture conditions and for each nacelle there are two of them that constitutes a redundancy in the rocket phase but that are both necessary to power the air compressor. The combustion chamber is also a relatively conventional component and in particular it uses a film cooling technique involving both the hydrogen and compressed air in the airbreathing phase and liquid oxygen in the rocket phase, since most part of the fuel is always already used to cool the helium loop. Other important components are the hydrogen and oxygen turbopumps which operates with inlet and outlet pressures respectively of 1 and 260 bar for the hydrogen turbopump in the airbreathing phase and 4 and 400 bar for the oxygen in the rocket phase. One key problem of this components is to avoid cavitation since it could damage the blades, conflicting with the Skylon requirement of being reusable and having a strict turnaround time. Regarding the helium loop, there is the circulator which is a centrifugal compressor that operates at almost constant speed and that is powered by the first hydrogen turbine.

To sum up, the SABRE is built for two relatively different purposes: to serve as an air breathing deeply precooled engine and as a high specific impulse rocket. In order to do so, it follows the cycle reported before and it comprises four thrust chambers, two preburner-HX3 units, two hydrogen turbopumps and two helium loops. This allows it to operate as one air-breathing engine and as two separate rocket engines. Thus, a key aspect of the models presented in the following chapter is that they are scaled down in order to incorporate one unit of each component and they neglect the presence of the ramjet burners, considering the intake to match the requests of the compressor with nominal pressure recovery. Therefore, the resulting performances are to be compared to one fourth of those of the full-scale engine, which still have to be doubled to match the Skylon propulsive plant characteristics, since it is made up of two SABRE.

2. Air-breathing models development

The models that will be presented are intended to be used during a conceptual design phase, in which different design choices must be made and compared nimbly in order to establish the best alternative. A path of increasing complexity was followed, in order to provide different models that can be chosen based on the level of knowledge of the design and amount of available data. The most complicated models are shown to give obviously better predictions but also the simplest ones gave results with good agreement with the data provided by Reaction Engines.

The first step in the development of these models was to establish a reference for the atmosphere, thus a standard atmospheric model derived from the International Standard Atmosphere had to be included in the code. The results are here plotted between 0 and 25 *km,* the altitude at which SABRE switches to the rocket mode and thus is not influenced by the atmosphere anymore. Then, the first and simplest model could be studied.

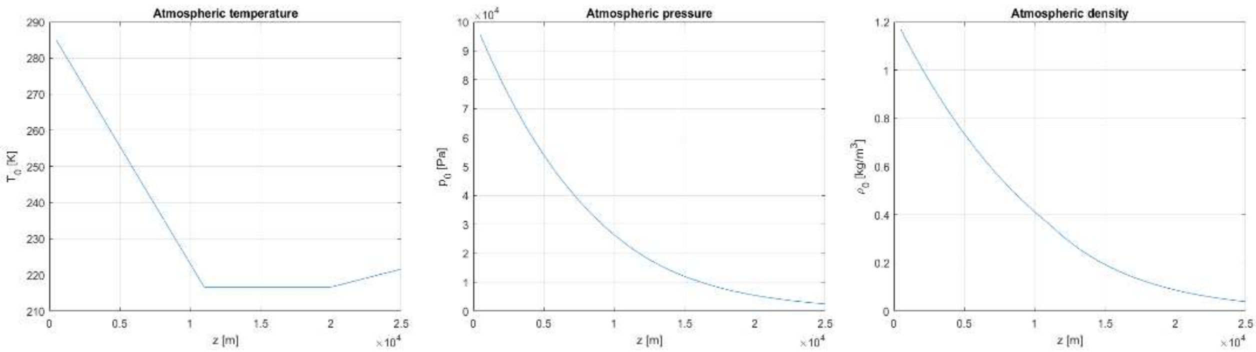

Figure 6 - Ambient characteristics at different altitude.

2.1 Ramjet with precooler and compressor

The simplest model that can be built, that is representative of what happens in the real thermodynamic cycle of the SABRE, considers only the air part of the cycle reported before. The simplified scheme is reported in Figure 7.

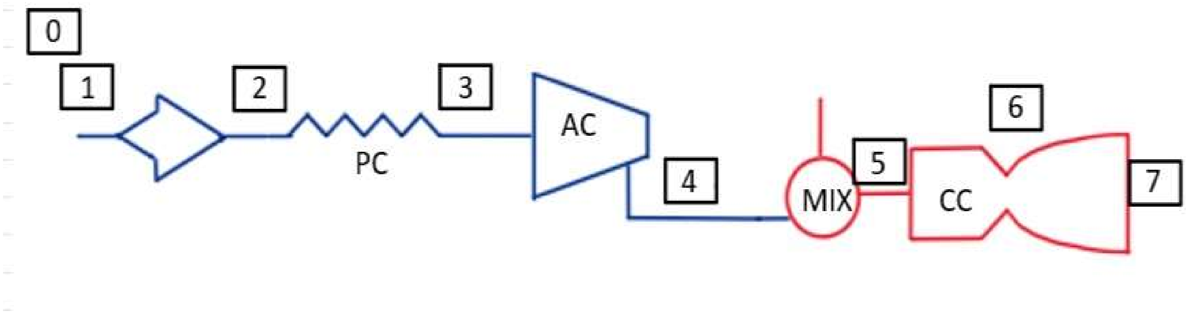

Figure 7 - Ramjet with precooler and compressor scheme.

Some hypothesis had to be stated in order to have a model as simple as possible and they are explained below where all the constitutive equations are presented. Assuming that in a first phase of the design neither the exact behavior of the intake is known nor the air mass flow captured and requested by the compressor, a constant mass flow equal to that at the design point is assumed. The intake is modeled as an adiabatic process through the total pressure recovery ratio $\epsilon_d = \frac{p_2^\circ}{p_1^\circ}$ which is calculated as suggested in [1] via the following equation

$$\epsilon_d = \left(1+0.5(\gamma-1)(1-\eta_k)M_0^2\right)^{(-\gamma/(\gamma-1))} \tag{1}$$

where η_k is the kinetic efficiency of the intake, which is the ratio of the kinetic energy of the outlet flow, if expanded isentropically to ambient pressure, to the free stream kinetic energy. This value was assumed equal to 0.9. The total temperature, calculated as in (2), is constant through the intake while the total pressure is obtained as in (3), with M_0 the free stream Mach number and γ the adiabatic expansion coefficient of air.

$$T^\circ_1 = T_0\left(1+\frac{\gamma-1}{2}M_0^2\right) \tag{2}$$

$$p^\circ_1 = p_0\left(1+\frac{\gamma-1}{2}M_0^2\right)^{\frac{\gamma}{\gamma-1}} \tag{3}$$

Regarding the precooler, the outlet temperature is considered as a design parameter and is always equal to 97K: this is equivalent to say that the PC is capable to adapt to the different demands in the different flight conditions and it is a sensible hypothesis given that in the real cycle the mass flow of hydrogen and the conditions of the helium loop can be adapted by using different valves. Instead, a total pressure loss of 28% is introduced, as done in [1].

The equations for the air compressor are the following:

$$p^\circ_4 = \beta_{AC}p^\circ_3 \tag{4}$$

$$T^\circ_4 = T^\circ_3\left(1+\frac{1}{\eta_{AC}}\left(\beta_{AC}^{\frac{\gamma_{34}-1}{\gamma_{34}}}-1\right)\right) \tag{5}$$

Where η_{AC}, β_{AC} and γ_{34} are respectively the adiabatic efficiency, the compression ratio and the average expansion coefficient of air between conditions 3 and 4.

Two key assumptions were made regarding the mixer: the gaseous hydrogen is fed at the same total pressure and temperature of the air and the amount of hydrogen is equal to the one giving a stoichiometric fuel ratio, $f=\frac{\dot{m}_{H2}}{\dot{m}_{air}}=f_{ST}=0.029$. The temperature at the end of the combustion is calculated as:

$$T^\circ_6 = T^\circ_5 + \eta_b\left(\frac{f_{ST}}{1+f_{ST}}\frac{H_i}{c_{p_{gas56}}}\right) \tag{6}$$

While the pressure is:

$$p^\circ_6 = \epsilon_b p^\circ_5 \tag{7}$$

Where $\eta_b=0.9$, $\epsilon_b=0.95$, f_{ST} is the stoichiometric fuel ratio, H_i is the lower calorific value of molecular hydrogen and $c_{p_{gas56}}$ is the weighted average specific heat between conditions 5 for the mixture and 6 for the combustion products. The pressure along the combustor is considered to be almost constant, considering a small loss of total pressure.

The most relevant hypothesis on the nozzle was for it to be always adapted. A pneumatic efficiency, that takes into account the total pressure losses due for example to viscosity effects near the walls, was introduced, as well as a nozzle efficiency which were conventionally put equal to respectively $\epsilon_n=0.98$ and $\eta_n=0.95$. The exit velocity is then evaluated with the following formula:

$$w_e = \sqrt{2c_{p_{gas6}}T_6^\circ\left(1-\beta^{\frac{\gamma_{gas6}-1}{\gamma_{gas6}}}\right)} \tag{8}$$

Where β is the ratio between the exit pressure and the total nozzle pressure that is equal to the total chamber pressure times the pneumatic efficiency. It is thus possible to calculate the following four figures of the engine (gross thrust, net thrust, specific impulse and specific thrust), using the input data in Table 1.

$$\begin{gathered} F_g=\eta_n \dot{m}_6 w_e \\ F_u=F_g-\dot{m}_1 u \\ I_{sp}=F_u/\dot{m}_{H2} \\ T_{sp}=F_u/\dot{m}_1 \end{gathered} \tag{9}$$

	Parameters	Value	Source	Notes
Preliminary	*Free stream Mach number* M_0	0-5	[5], from REL	
	z, altitude	0-25000 m	[5], from REL	
	Air mass flow, $\dot{m}_1$	90.1 kg/s	[5]	supposed constant
Intake	*Intake kinetic efficiency*, η_k	0.9	[5]	
Precooler	*PC pneumatic efficiency*, ϵ_{PC}	72%	[5]	supposed constant
	PC outlet temperature, $T°_3$	97K	[5]	supposed constant
Air compressor	*AC efficiency* η_{AC}	0.8		Assumption
	AC pressure ratio β_{AC}	122	[5]	supposed constant
CC	*Combustion efficiency* η_b	0.9		Assumption
	Pneumatic combustor efficiency ϵ_b	0.95		Assumption
	Lower calorific value H_i	120.9e6 J/kg		
Nozzle	*Pneumatic efficiency* ϵ_n	0.98		Assumption
	Nozzle efficiency η_n	0.95		Assumption

Table 1 - Input data for the ramjet with precooler and compressor model

2.2 Complete air cycle

As it can be seen in Figure 8, this model introduces some new elements such as the pre-burner and secondary heat exchanger, but it still does not take into consideration the auxiliary cycles of helium and hydrogen.

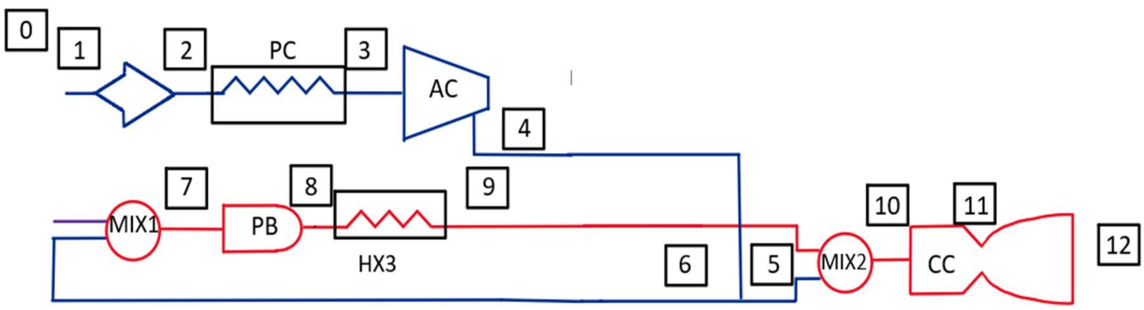

Figure 8 - Complete air cycle scheme.

In this model, the intake is described via the real characteristics of the SABRE intake, as reported in [1]. The total pressure recovery factor is reported in Figure 9, for varying Mach number and altitude.

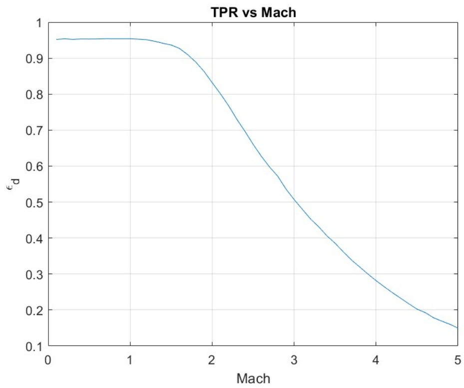

Figure 9 - total pressure recovery of the real intake along the trajectory.

The precooler and compressor have the same behavior as described previously and the air is supposed to be split in half in the node between the pre-burner and main combustion chamber, as reported both in [1] and [3]. In the first mixer the total amount of hydrogen needed by the engine is mixed with half of the air ingested: this could be enough to consider the mixture rich in fuel, but in addition to this it must be noted that the SABRE runs with an overall fuel to air ratio higher than the stoichiometric ratio, for reasons related to the cooling of the incoming air. Thus, in this model the real fuel equivalence ratio was used, differently from the previous model where this parameter was set to 1. In particular, as it will be seen later, this model was used to evaluate the results in two different cases: the first one in which the parameters are considered constant and equal to the design point values as before, in order to see the influence of the non-adapted nozzle and of the pre-burner; in the second case the parameters were varied along the trajectory according to the data published by Reaction Engines Ltd or reported in [5]. In particular, regarding the equivalence ratio Φ, it varies linearly along the ascent from 2.5 to 2.8, that is the design point value. Regarding the hydrogen total temperature and pressure, as before, they were assumed to be equal to those of the air in station 4. This is verified by the fact that also in [5] the values of air and hydrogen are nearly equal. In the pre-burner the rich mixture is burnt. In order to evaluate the outlet temperature, it is assumed that all the air burns with an amount of hydrogen corresponding to the one that gives a stoichiometric fuel ratio. Thus, in the outlet the composition will be a mixture of nitrogen, unburnt hydrogen and water vapor at high temperature and pressure, disregarding the reactions between hydrogen and nitrogen. The exit temperature and pressure are thus evaluated as follows:

$$T°_8 = T°_7 + \eta_b \frac{f_{ST}}{1+f_{PB}} \frac{H_i}{c_{p_{78}}} \tag{10}$$

$$p°_8 = p°_7 \epsilon_b \tag{11}$$

where η_b, ϵ_b are defined as before and $f_{PB} = \dot{m}_H / \dot{m}_6$.

Regarding HX3, an assumption like that made for the precooler was made, thus considering the outlet temperature constant and equal to the design value, that was taken from [5]. Regarding the total pressure instead, it was assumed to remain constant along the flow through the heat exchanger, in a similar manner to what is done in [10]. In the second mixer it is necessary to evaluate both the thermophysical properties of the outlet mixture, which will be composed by the same elements described before with the added fresh air, and also the outlet temperature and pressure conditions. In the combustion chamber the mixture is once again rich in hydrogen thus the same hypothesis made for the pre-burner is made here, considering that only a fraction of the hydrogen corresponding to the stoichiometric fuel ratio burns; the equations are not reported since they are analogous to (10) and (11). Regarding the nozzle, it is here considered non-adapted. First of all, $p°_{12} = p°_{11} \epsilon_n$, where the nozzle pneumatic efficiency is the same as before. Then the nozzle area ratio at separation, AR, needs to be known. It is computed in [5], by applying the Summerfield criterion, that is to say that the jet detaches from the nozzle wall when the pressure is as low as the 30% of the ambient pressure. The values are assumed to be the same here and the plot of the AR along the trajectory is here reported.

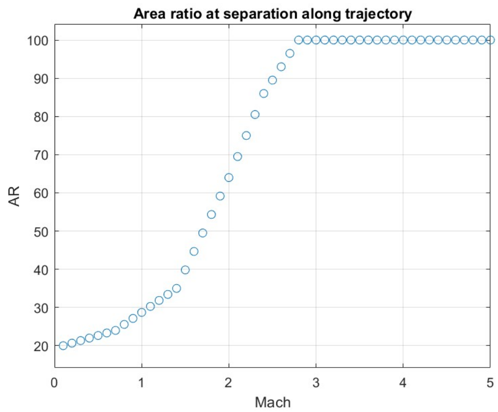

Figure 10 - area ratio at separation along the trajectory.

As can be seen the flow separates inside the nozzle until the free stream Mach number is almost 3: after this point the nozzle runs full but the flow is still over-expanded until it reaches M=4.5 at 23 km of altitude. This datum was used to estimate the nozzle throat area through the following equation which is the equation for the mass flow in the throat assuming that the flow is sonic.

$$A_t= \dot{m}\,\frac{\sqrt{R_{gas}T_{11}^{\circ}}}{\sqrt{\gamma_{gas11}{*}p_{11}^{\circ}}}\left(1+\frac{\gamma_{gas11}-1}{2}\right)^{\frac{\gamma_{gas11}+1}{2\left(\gamma_{gas11}-1\right)}}=0.0122m^2 \tag{12}$$

Now it is possible to calculate the area at separation: $A_{sep}=ARA_t$.

The other variable that needs to be known is the ratio between the exit and chamber pressure β, that appears in the equation:

$$w_e=\sqrt{2c_{p_{gas11}}T_{11}^{\circ}\left(1-\beta^{\frac{\gamma_{gas11}-1}{\gamma_{gas11}}}\right)} \tag{13}$$

used to calculate the exit velocity, where, differently from before, it is not possible to calculate the ratio assuming $p_e=p_0$. In order to do so, the following equation of the mass flow at the separation area had to be solved iteratively using Newton's method:

$$\sqrt{\beta^{\frac{2}{\gamma_{gas11}}}-\beta^{\frac{\gamma_{gas11}+1}{\gamma_{gas11}}}}-\dot{m}_{10}\frac{\sqrt{R_{gas}T_{11}^{\circ}}}{p_{11}^{\circ}A_{sep}}\sqrt{\frac{\gamma_{gas11}-1}{2\gamma_{gas11}}}=0 \tag{14}$$

It is now possible to calculate the performance parameters as done before.

	Parameters	Value	Source	Notes
Preliminary	*Free stream Mach number* M_0	0-5	[5], from REL	
	Altitude z	0-25000m	[5], from REL	
	Air mass flow $\dot{m}_1$	90.1 kg/s	[5]	supposed constant
Intake	*Intake total pressure recovery* ϵ_d	0.15–0.95	[5]	
Precooler	*PC pneumatic efficiency,* ϵ_{PC}	72%	[5]	supposed constant
	PC outlet temperature, T°_3	97K	[5]	supposed constant
Air compressor	*AC efficiency* η_{AC}	0.8		Assumption
	AC pressure ratio β_{AC}	122 kg/s	[5]	supposed constant
Node CC-PB	$\frac{\dot{m}_{PB}}{\dot{m}_{tot}}$	0.5	[5]	supposed constant
Mixer 1	*fuel/air equivalence ratio* Φ	2.8	[5], from REL	supposed constant
Pre-burner	*Combustion efficiency* η_b	0.9		Assumption

	Pneumatic efficiency ϵ_b	0.95		Assumption
	Lower calorific value, H_i	120.9e6 J/kg		
HX3	*Outlet total temperature $T°_9$*	1174	[5]	supposed constant
Nozzle	*Pneumatic efficiency ϵ_n*	0.98		Assumption
	Efficiency η_n	0.95		Assumption
	Area ratio at separation AR	20-100	[5]	

Table 2 - Input data for the complete air cycle model

As said before, the model was tested in two different cases: one in which the air mass flow, the AC pressure ratio and the fuel to air equivalence ratio are constant, as reported in the table above, and one in which are variable, according to the trends reported in [5], with values comprised in the ranges reported in Table 3 for these values.

2.3 Complete model

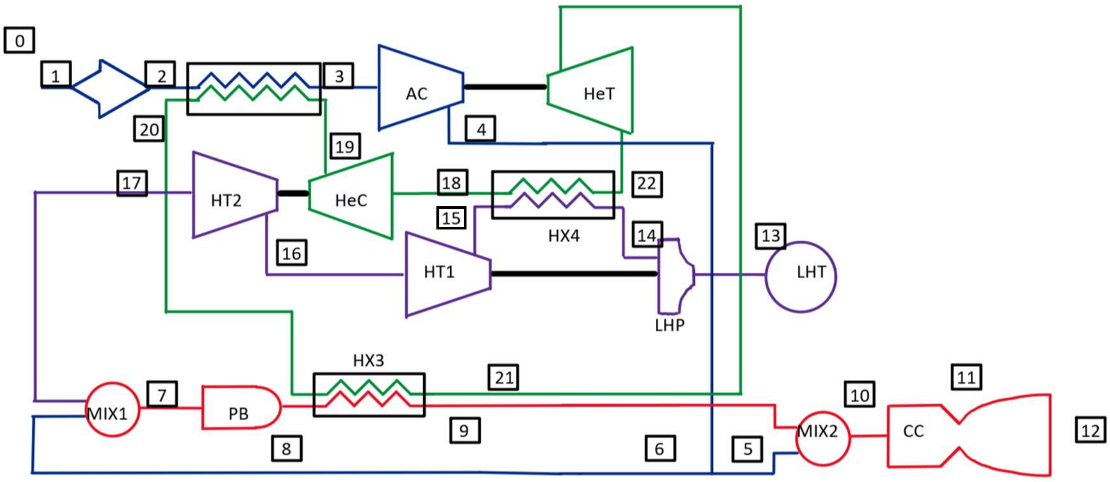

Figure 11 - Complete model scheme.

The most complete and complicated model is represented in Figure 11, where also the hydrogen and helium cycle are included. The path followed for the calculation in this model is slightly different. The behavior of the intake, precooler and air compressor is the same described in 2.2. Then, the helium turbine was solved. First, it was necessary to have the helium mass flow $\dot{m}_{He}$ that was set equal to 22 kg/s, as in [5]. As indicated in [10], the helium turbine inlet temperature was considered a constant design parameter equal to 1190K. Then the following equations were used:

$$W_{HeT}=-W_{AC} \tag{15}$$

$$T°_{22}=T°_{21}+W_{HeT}/\left(c_{p_{He}}\,\dot{m}_{He}\right) \tag{16}$$

$$\beta_{HeT}=\left(\frac{1}{\eta_{HeT}}\left(\frac{T°_{22}}{T°_{21}}-1\right)+1\right)^{\frac{-\gamma_{He}}{\gamma_{He}-1}} \tag{17}$$

Where the first one is the power balance between the air compressor and helium turbine, disregarding mechanical efficiencies, the helium specific heat and expansion coefficient were considered constant as done in [4] and the last one is the relation between temperatures and pressure ratio in the turbine β_{HeT}.

The helium compressor inlet temperature was set to a constant value of 50 K, as in [5], thus allowing to calculate the varying exchanged heat Q_{HX4} along the trajectory:

$$Q_{HX4}=\dot{m}_{He}c_{p_{He}}(T°_{18}-T°_{22}) \tag{18}$$

Then, as done in [10] the pressure was considered constant through HX4.

Since in all heat exchangers total pressure could be assumed to remain unchanged, as done by [10] and showed by [5], the pressure ratio in the compressor must be the same of the turbine, in order to have congruence of pressures in the helium cycle. Thus $\beta_{HeC}=\beta_{HeT}$. Then:

$$T_{19}°=T°_{18}\left(1+1/\eta_{HeC}\left(\beta_{HeC}^{\frac{\gamma_{He}-1}{\gamma_{He}}}-1\right)\right) \tag{19}$$

$$W_{HeC}=\dot{m}_{He}c_{pHe}(T°_{19}-T°_{18}) \tag{20}$$

$$p°_{19}=p°_{18}\beta_{HeC} \tag{21}$$

Given the heat exchanged Q_{PC} calculated before in the air side of the precooler, it is possile to write

$$T°_{20}=T°_{19}-Q_{PC}/\left(\dot{m}_{He}c_{p_{He}}\right) \tag{22}$$

It is now possible to estimate the heat exchanged in HX3 along the ascent, which in the previous model was calculated considering a constant outlet temperature on the air side.

$$Q_{HX3}=\dot{m}_{He}c_{p_{He}}(T°_{21}-T°_{20}) \tag{23}$$

Moving to the hydrogen cycle, the following path was followed.

The conditions at the tank outlet are considered constant and the values were taken from [5]. In order to maintain simplicity, constant specific heats and specific heat ratio were assumed with a value corresponding to an average of the conditions in the cycle ($c_{p_H}=14600J/kgK$, $c_{v_H}=10290J/kgK$, $\gamma_H=1.42$).

The fuel to air equivalence ratio Φ was chosen, as done before, to vary linearly from 2.5 to 2.8 along the ascent, thus it was possible to calculate the hydrogen mass flow $\dot{m}_H=\Phi f_{ST}\dot{m}_1$ where f_{ST} is the stoichiometric fuel ratio equal to 0.029.

Given the conditions reported in [5], while flowing in the turbopump the hydrogen passes from liquid to supercritical state, while according to those calculated in [10], the hydrogen remains in the liquid state. Here, for the sake of simplicity the hydrogen was considered liquid and an average density of $73kg/m^3$ was assumed. Then a pressure ratio of the turbopump of 257, equal to the value at design point in [5] was chosen and assumed constant during the ascent. It was then possible to calculate the outlet pressure and the power consumed by the turbopump, using an efficiency $\eta_{LHP}=0.8$.

$$p°_{14}=p°_{13}\beta_{LHP} \tag{24}$$

$$W_{LHP}=\dot{m}_H\frac{p°_{14}-p°_{13}}{\eta_{LHP}\rho_{LH}} \tag{25}$$

$$T°_{14}=T°_{13}+\frac{1-\eta_{LHP}}{\eta_{LHP}}\frac{W_{LHP}}{\dot{m}_Hc_H} \tag{26}$$

After exiting the pump, the hydrogen flows in the heat exchanger where part of the heat extracted by the helium in the precooler is given off to the hydrogen stream. The exit temperature can be calculated as:

$$T°_{15}=T°_{14}-Q_{HX4}/\left(\dot{m}_Hc_{p_H}\right) \tag{27}$$

Passing to the first hydrogen turbine, the power produced was set equal to that necessary to the turbopump, neglecting once again the mechanical efficiencies while the turbine efficiency was set to 0.8.

$$W_{HT1}=-W_{LHP} \tag{28}$$

$$T°_{16}=T°_{15}+W_{HT1}/\left(\dot{m}_H c_{p_H}\right) \tag{29}$$

$$\beta_{HT1}=\left(\left(\frac{T°_{16}}{T°_{15}}-1\right)/\eta_{HT1}+1\right)^{-\gamma_H/(\gamma_H-1)} \tag{30}$$

$$p°_{16}=p°_{15}\beta_{HT1} \tag{31}$$

Regarding the second hydrogen turbine, first a turbine efficiency of 0.8 was assumed and the balance of power with the helium compressor was written, neglecting the mechanical efficiencies and then the same procedure used for HT1 was followed, getting as a result the pressure and temperature at the inlet of the first mixer:

$$W_{HT2}=-W_{HeC} \tag{32}$$

$$T°_{17}=T°_{16}+W_{HT2}/\left(\dot{m}_H c_{p_H}\right) \tag{33}$$

$$\beta_{HT2}=\left(\left(\frac{T°_{17}}{T°_{16}}-1\right)/\eta_{HT2}+1\right)^{-\gamma_H/(\gamma_H-1)} \tag{34}$$

$$p°_{17}=p°_{16}\beta_{HT2} \tag{35}$$

Regarding the remaining components, they were treated as in the complete air cycle model, in particular with a non-adapted nozzle.

	Parameters	Value	Source	Notes
Preliminary	*Free stream Mach number M_0*	0-5	[5], from REL	
	Altitude z	0-25000m	[5], from REL	
	Air mass flow $\dot{m}_1$	77.3 - 92 kg/s	[5]	
Intake	*Intake total pressure recovery ϵ_d*	0.15-0.95	[5]	
Precooler	*PC pneumatic efficiency,ϵ_{PC}*	72%	[5]	supposed constant
	PC outlet temperature, $T°_3$	97K	[5]	supposed constant
Air compressor	*AC efficiency η_{AC}*	0.8		Assumption
	AC pressure ratio β_{AC}	65 - 180	[5]	
Liquid Hydrogen Tank	*fuel/air equivalence ratio Φ*	2.5 - 2.8	[5], from REL	
	Tank temperature $T°_8$	18 K	[5]	
	Tank pressure $p°_8$	1 bar	[5]	
Liquid Hydrogen Pump	*Efficiency η_{LHP}*	0.8		Hypothesis
	LHP compression ratio β_{LHP}	257	[5]	Supposed constant
Hydrogen turbine	*Efficiency η_{HT1}*	0.8		Assumption
Helium turbine	*Efficiency η_{HeT}*	0.8		Assumption

	Turbine inlet temperature $T°_{21}$	1190 K	[5]	constant
Helium compressor	*Compressor inlet temperature $T°_{18}$*	50 K	[5]	Supposed constant
	Compressor efficiency η_{HeC}	0.8		Assumption
Node CC-PB	$\frac{\dot{m}_{PB}}{\dot{m}_{tot}}$	0.45-0.6		
Pre-burner	*Combustion efficiency η_b*	0.9		Assumption
	Pneumatic efficiency ϵ_b	0.95		Assumption
	Lower calorific value, H_i	120.9e6 J/kg		
Nozzle	*Pneumatic efficiency ϵ_n*	0.98		Assumption
	Efficiency η_n	0.95		Assumption
	Area ratio at separation AR	20-100	[5]	

Table 3 - Input data for the complete model

2.4 Results

The performance parameters were calculated and plotted along all the ascent trajectory, from Mach 0 to Mach 5 and from 0 km to 25 km. The results were then compared to the data published by Reaction Engines, which were reported in [5], and, for example for the gross thrust, an error was calculated as:

$$err_{F_g} = \frac{F_g - F_{g_{REL}}}{F_{g_{REL}}} \tag{36}$$

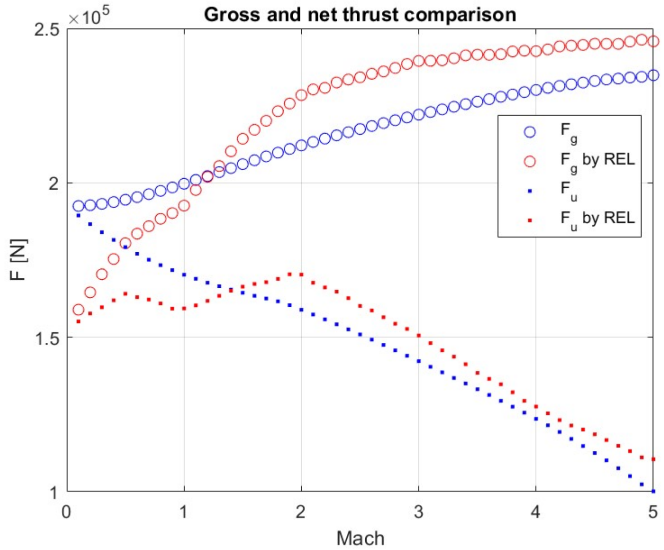

Figure 12 - Gross and uninstalled thrust comparison for the ramjet with precooler and compressor model.

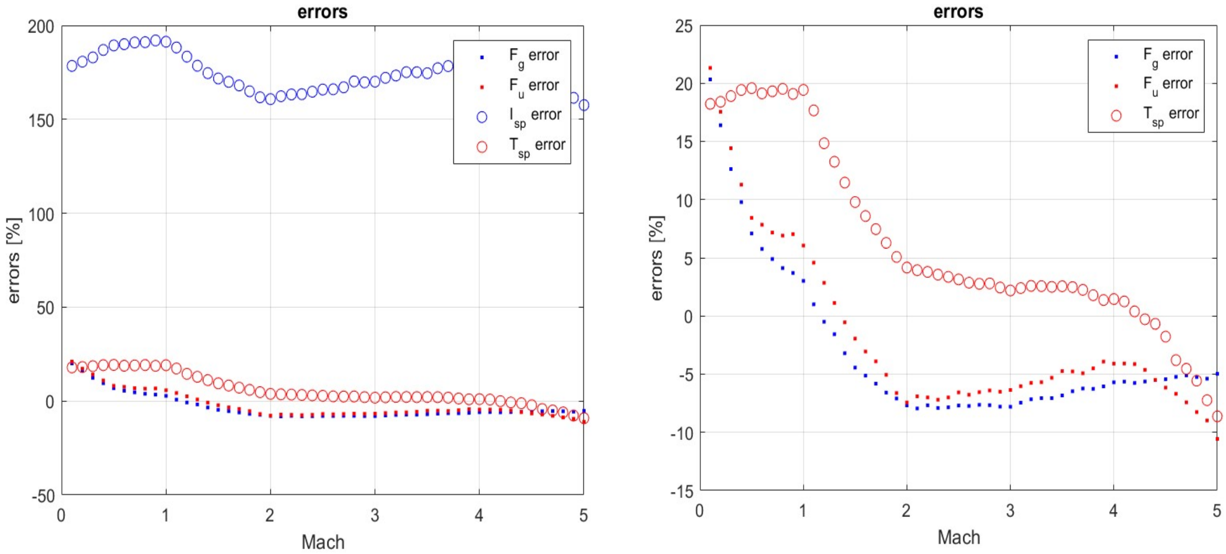

Figure 13 - Errors for the ramjet with pre-cooler and compressor model.

As it can be seen in the graphs in Figure 13, the first model behaves well in predicting the thrust and specific thrust, especially in the later part of the trajectory: this is due to the fact that in the real engine, after the initial phase the parameters reach the design point values that were used here to obtain the results. In particular, the maximum absolute value of the errors for the gross, net and specific thrust are respectively 20.33%, 21.31% and 19.56%. Despite these results, the model fails completely in predicting the specific impulse. This is due to the assumption made regarding the fuel ratio: it was here assumed that it was equal to the stoichiometric fuel ratio, but it is well established that the SABRE runs with a rich mixture of air and hydrogen in order to accomplish the cooling aspects with the auxiliary cycles of hydrogen and helium that here were completely discarded. This in turn affects the specific impulse giving a maximum error of 193%. This problem was addressed in the other models.

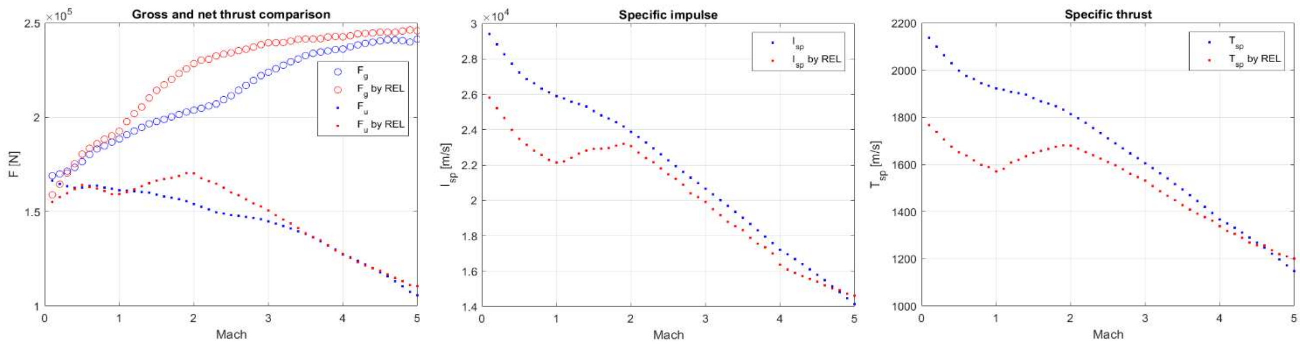

Figure 14 - Gross and uninstalled thrust, specific impulse and specific thrust comparison for the complete air cycle model.

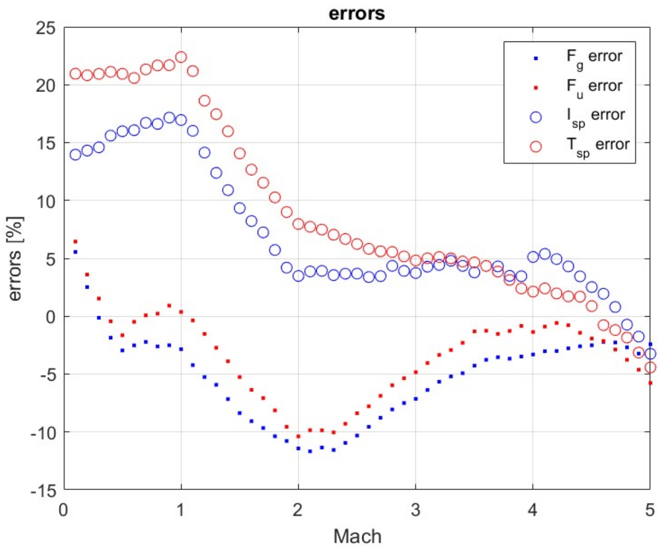

Figure 15 - Errors in the complete air cycle with variable parameters.

The most notable difference between the second model (Figure 15) and the one before is the error on the specific impulse: here the real equivalence ratio was used and this has a huge influence on this performance parameter and the maximum absolute value of the error is 17.45%. Regarding the gross and uninstalled thrust, this model also improves their prediction since maximum error is now 11.5% and 10.14% while the previous ones were almost double. Regarding the specific thrust there is a slight increment in the maximum error that reaches 22.7%. However, it must be noted that in the previous model, in the first part of the trajectory the mass flow was higher than the real value thus taking the calculated curve for the specific thrust closer to the one published by REL. This does not happen here, giving then the higher error: this is linked to the fact that the values used for the mass flow are not directly published by REL, whose data are usually hard to find or not available, but are based on the previous calculations made by [1] and can be affected by errors.

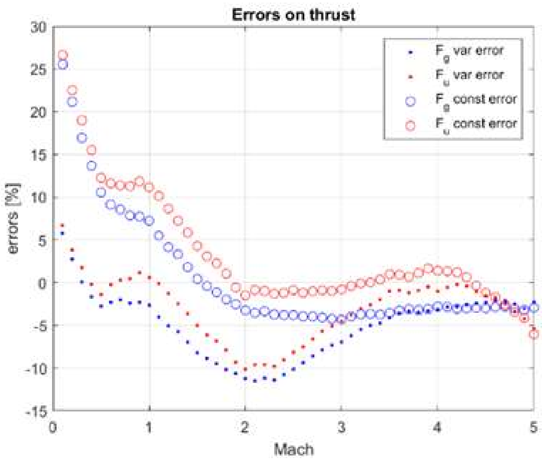

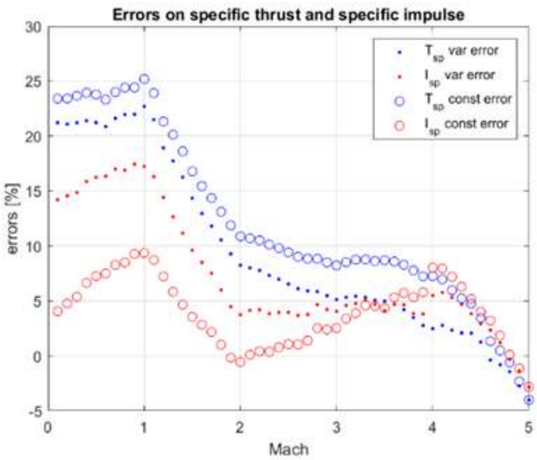

Figure 16 - comparison between the complete air cycle model with variable and constant parameters.

By comparing the complete air cycle model with constant and variable parameters (Figure 16), it can be noted that the accuracy of the two cases in predicting the net, gross and specific thrust is similar while the model with constant parameters behaves better in predicting the specific impulse in the first phase, even if this is due to the higher amount of hydrogen considered in this phase, in which also the ramjet burners, that are here not considered, are active.

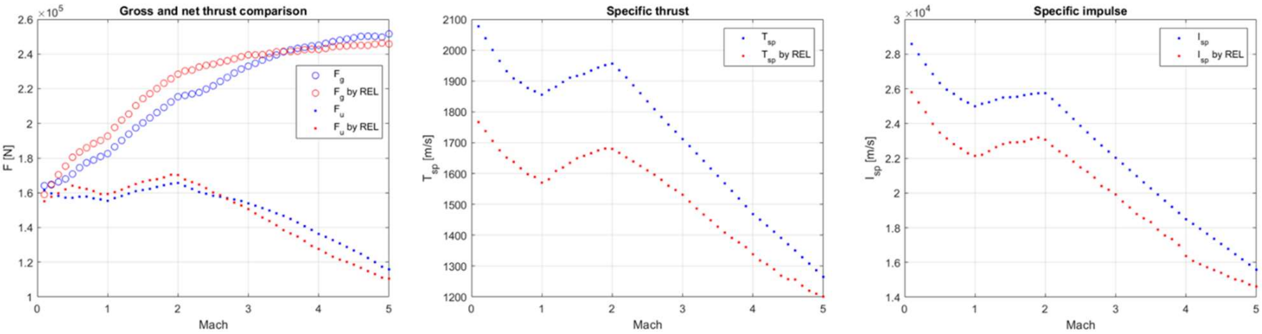

Figure 17 - Results comparison for the complete model

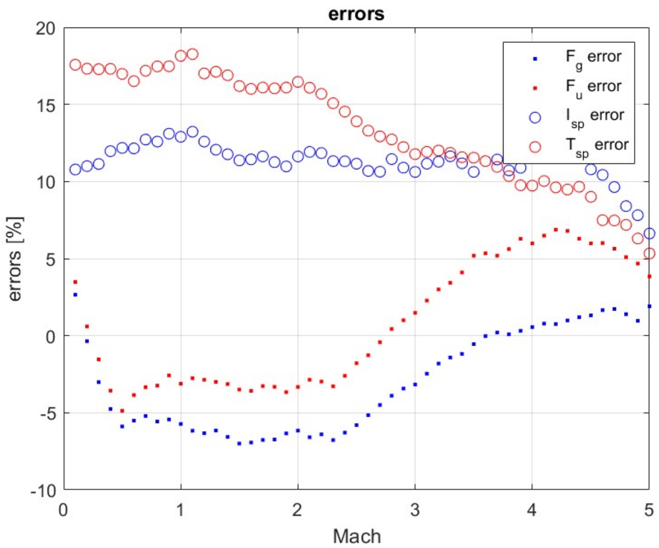

Figure 18 - Errors in the complete model.

As it can be noted, in the complete model the errors in Figure 18 are lower: in fact, the maximum error for the gross thrust is a negative 7% while for the net thrust is 6.9%. Also, the maximum error on the specific impulse and thrust are lower and respectively of 13.2% and 18.3%. However, apart from the higher precision, the main advantage of this model is its capability of giving an insight of what happens in the helium and hydrogen cycles, that were previously neglected, thus allowing for a more complete understanding of the functioning of the engine. This is paid with a much higher request of input parameters that are necessary to run the model, thus it can be used only in a phase in which the design of the engine is already advanced.

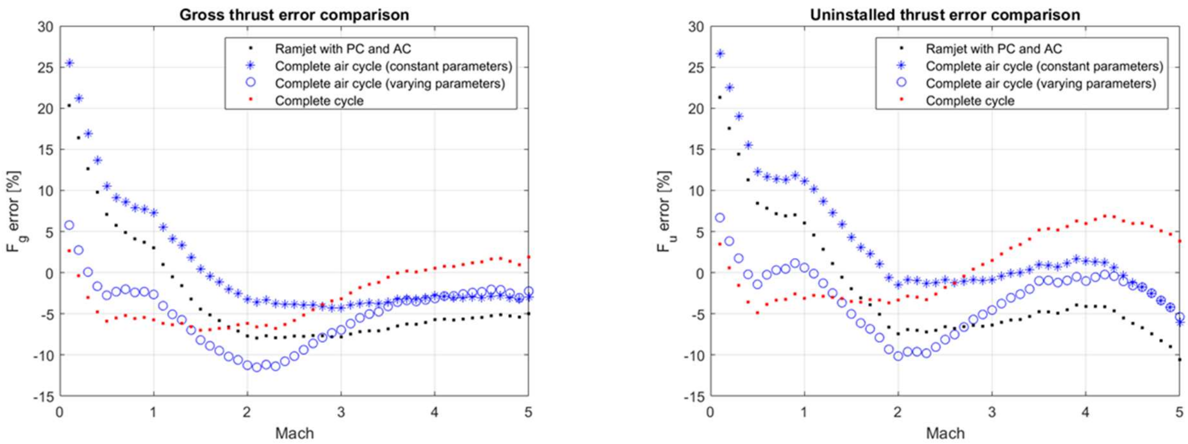

Figure 19 - Comparison of the errors of gross and net thrust of all the models.

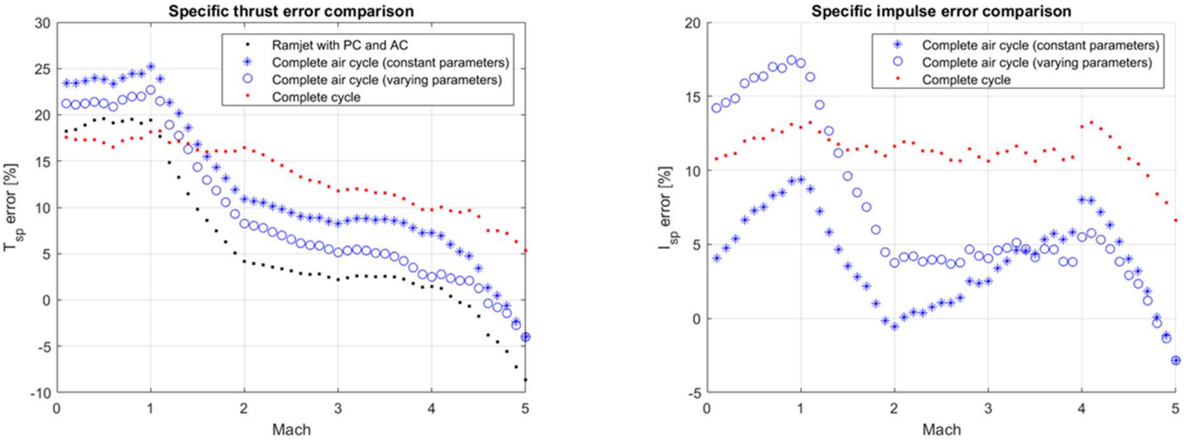

Figure 20 - Comparison of the errors of specific thrust and impulse of all the models.

From Figure 20, regarding the gross thrust, it is possible to see that the ramjet with precooler and compressor model and the complete air cycle with constant parameters model give rise to similar trends for the errors, showing that they are highly inaccurate in subsonic flight. At high Mach flight, all the models give similar results thus showing that in a context in which only on design performance are desired the simpler models can be satisfying. In a wide Mach range however, the complete cycle model is the one giving the best results. Taken the net thrust, similar considerations can be made and in particular it is interesting how, at high Mach numbers, the complete model gives rise to higher errors with respect to the other, even if it is generally better along all the design space. Looking at the specific thrust in Figure 20, all the models show similar trends and while the complete model is better at low Mach numbers, the simpler models are better again at the end of the ascent. Coming to the specific impulse, the results of the first model are not shown because, as explained before, they are completely out of scale. Regarding the other models, the complete air cycle with constant parameters should not be considered because its results are affected by the assumption of using constant fuel flow equal to the value at the design point which is the highest. Then, from a first look at the two remaining curves, it could appear that the complete air cycle model is better. However, this is due to the fact that all the models over-estimate the specific impulse and since the air cycle model underestimates the uninstalled thrust the distance between the calculated specific impulse and the real one is lower, thus giving lower errors than the complete model.

3. Conclusions

As it was shown in 2.4, all the models show good agreement with the available data and, with the increasing complexity of the model, better results can be obtained. However, this is done by requiring also more precise and numerous input data which are not always available. Thus, the choice of the model to be applied depends essentially on the stage of the design that is intended to be studied. The simplest model comprises only indispensable elements of the engine and introduces many simplifying hypothesis (though giving good results especially at high Mach numbers, close to the design point), that are gradually dismissed in the other models, increasing both the calculation complexity and especially the number of required input data, that sometimes had to be hypothesized due to the lack of literature regarding the topic. Along with the three models here described, another one was created and it was essentially an attempt of including the fuel cycle, without considering the helium cycle. This lead to increase the complexity and the input data number without appreciable improvements in the results, which is the reason why it is not shown here. This is due to the fact that it described an engine substantially different from SABRE, which uses helium in order to avoid problems of hydrogen embrittlement in the precooler.

All the models here presented were then coded in a Matlab Graphical User Interface, in order to be readily usable, even without knowing the code and can be added in ASTRID-H, a conceptual design tool developed at Politecnico di Torino to estimate high-speed vehicles characteristics [11].

In future iteration, a desirable improvement could be a better modeling of the combustion, even with chemical simulations of the combustor, that can also be used to assess the environmental compatibility of the engine, exploiting the complete model which gives accurate predictions of temperatures and pressures at each stage. The emission of both greenhouse gases and pollutant species such as NO_x were already estimated by the author, proving the low environmental impact of SABRE but will be subject of more accurate analysis in the near future.

4. Contact Author Email Address

mailto: s305110@studenti.polito.it

Giovanni Grimaldi

Address: Strada Tetti Bona 12, 12042 Bra (CN), Italy

Mobile phone: +39 3388014497

5. Copyright Statement

References

[1] M. Hempsell, B. Gallagher , J. Aprea and G. Sadlier, "A Business Analysis of a SKYLON-based European Launch Service Operator," *Acta Astronautica,* no. 121, pp. 1-12, 2016.

[2] R. Varvill, F. Jivraj and G. Paniagua, "The Scimitar Precooled Mach 5 Engine," in *2nd European Conference for Aerospace Sciences*.

[3] Reaction Engines Limited, "Skylon Users' Manual," 2014.

[4] T. Tanbay, M. Bisar Uca and A. Durmayaz, "Assessment of NOx emissions of the Scimitar engine at Mach 5, based on a thermodynamic cycles analysis.," *International Journal of Hydrogen Energy,* no. 45, pp. 3632-3640, 2020.

[5] V. Fernandez-Villace, *Simulation, design and analysis of air-breathing combined-cycle engines for high speed propulsion,* Madrid: Universidad Politécnica de Madrid, 2013.

[6] TEC-MPC, ESA, "Skylon Assessment Report," 2011.

[7] R. Varvill, "Heat exchanger development at Reaction Engines Ltd.," *Acta Astronautica,* no. 66, pp. 1468-1474, 2010.

[8] Reaction Engines Limited, "Reaction Engines," [Online]. Available: www.reactionengines.co.uk.

[9] D. Jian and Z. Qiuru, "Key technologies for thermodynamic cycle of precooled engines: A review," *Acta Astronautica,* no. 177, pp. 299-312, 2020.

[10] J. Zhang, Z. Wang and Q. Li, "Thermodynamic efficiency analysis and cycle optimization of deeply precooled combined cycle engine in the air-breathing mode," *Acta Astronautica,* no. 138, pp. 394-406, 2017.

[11] D. Ferretto, N. Viola and R. Fusaro, "A conceptual design tool to support high-speed vehicle design," in *AIAA Aviation 2020*, 2020.

[12] National Institute of Standards and Technology, Thermophysical properties of fluid systems.

[13] O. Nailard, "Eliminating the boundary between sky and space," *Physics World,* no. 33, 2020.

[14] UK Parliament, "Written evidence from Reaction Engines Limited," London, 2011.

[15] J. N. Pelton, *Space 2.0: Revolutionary Advances in the Space Industry*, Springer, 2019.